www.cadanda.com Computer-Aided Design AND APPLICATIONS

Analysis and Evaluation of Limb Alignment in Total Knee Replacement

Nilesh Ghongade[1], Ravi Warkhedkar[2] and Ashok Shyam[3]

[1]Government College of Engineering, nileshghongade@gmail.com
[2]Government College of Engineering, raviwar@indiatimes.com
[3]Indian Orthopaedics Research Group, drashokshyam@yahoo.co.uk

ABSTRACT

Numerous factors contribute to success of a total knee replacement (TKR); including surgical instruments, operational methods, positioning of prosthesis, cementing techniques, surgical experience and limb alignment. Limb alignment of $\pm 3^0$ has been rationally thought to be an acceptable alignment and clinical studies have to certain extent validated these assumptions. However these alignment boundaries still remain a hypothesis, as $\pm 3^0$ is an arbitrary value; therefore need validation. In this work, the main objective was to analyze the pattern of relative stress distribution in TKR if the axial alignment is gradually increased or decreased including the range of $\pm 3^\circ$. This work shows an application of digital modeling of limbs and implants, where CAD has been applied to design and assembly of femur, tibia and knee implants. The analysis was carried out at different alignment positions in Ansys workbench 14.0. It was found that within $\pm 4^\circ$ the rise in stress across the model surfaces is not much, however beyond $\pm 5^\circ$ there is dramatic increase in pressure and pressure imbalance with every degree of change. This investigation will be useful for surgeons in TKR surgeries and possibly underlines the importance of use of computer assisted surgeries to obtain more accurate alignment and more ever to avoid the outliers outside $\pm 5^\circ$ which might cause grater imbalance and early failure of implants.

Keywords: total knee replacement, limb alignment, point cloud technique, 3D reconstruction, finite element analysis.

1. INTRODUCTION

1.1. Total Knee Replacement (TKR)

Osteoarthritis remains one of the most widely diagnosed and threatening condition to stifle stability and knee functions in human being. Total knee replacement is the most frequent surgery done for end stage osteoarthritis of the knee and remains one of the most successful surgeries in history of orthopaedics. The surgery consists of replacing the diseased or damaged joint surfaces of the knee with metal and polyethylene components shaped to allow continued motion of the knee as shown in Fig. 1. Knee replacement surgery was first performed in 1968. Since then, improvements in surgical materials and techniques have greatly increased its effectiveness.

Successful knee replacement surgery involves implanting artificial components with such precision that the hip-knee-ankle axis is aligned to efficiently transfer the patient's weight to the ground without producing any undue stress on the bone [2]. The technical objective of total knee replacement surgery is to replicate this 'new' alignment and it is achieved during the surgery through precise and orchestred surgical steps [1,18].

1.2. Alignment

The mechanical axis of limb is made of axis of femur and tibia. Femoral mechanical axis (FMA) is a straight line drawn from the femoral head to the middle of intercondylar region and tibial mechanical axis (TBA) from tibial plateau to center of ankle joint as shown in Fig. 2 (a) [4,10,15]. Both normally aligned mechanical axes represent the straight line drawn from the center of the femur head to the center of the ankle. It passes through the center of intercondylar region of the knee i.e. entire limb in standing position from hip to ankle which is also considered as load bearing axis (LBA) of the body. Overall alignment is the angle made by femoral axis with the tibial axis in the coronal plane [17]. This can be maintained by computer navigation system or a reference line drawn on the skin from hip to ankle [11].

Taylor & Francis
Taylor & Francis Group

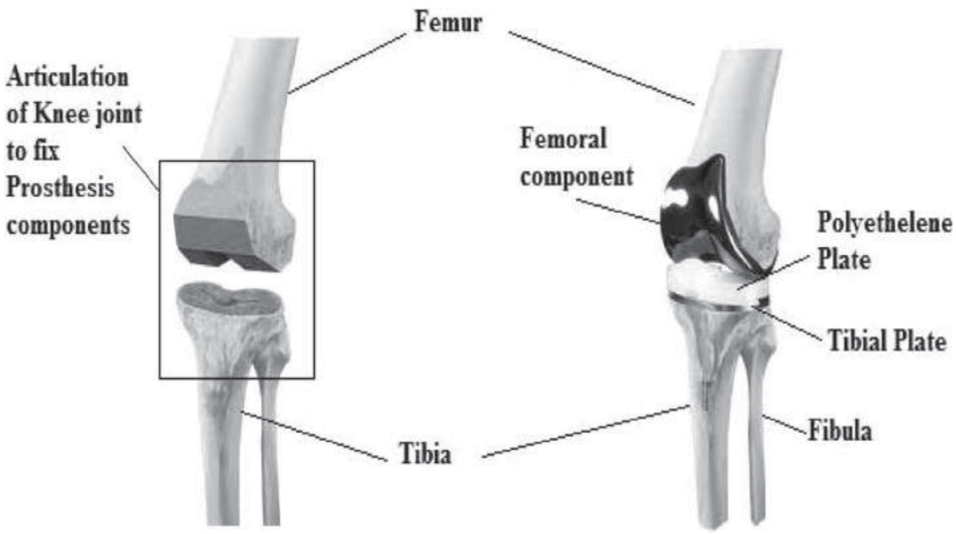

Fig. 1: Total knee replacement.

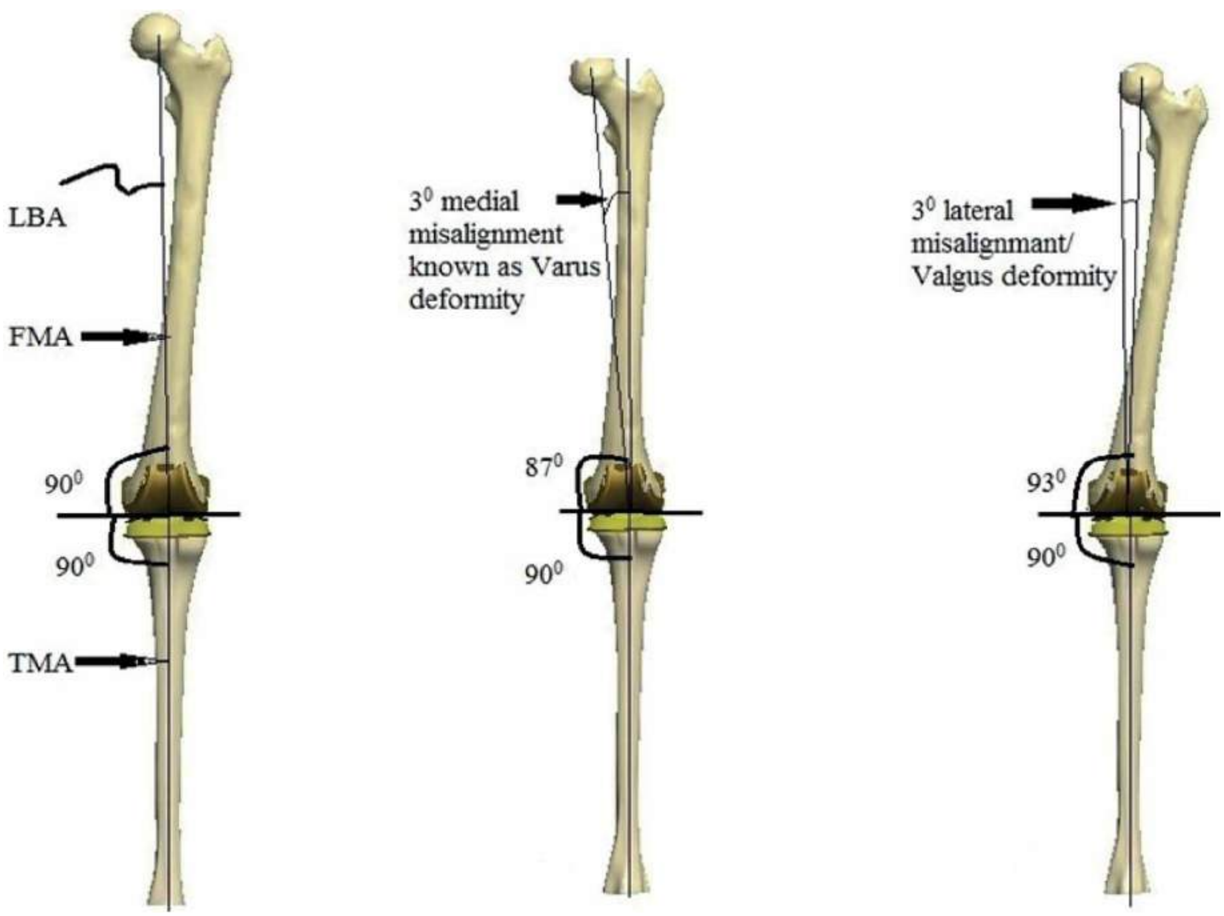

Fig. 2: (a) Coronal plane view of normal limb alignment after TKR showing load bearing axis (LBA) which passes from femoral head to center of ankle through replaced knee center. LBA is obtained by joining the femoral mechanical axis (FMA) and tibial mechanical axis (TBA). (b) 3^0 medial deflection of FMA disturbing normal LBA, known as varus deformity. (c) 3^0 lateral deflection of FMA disturbs normal LBA, which known as varus deformity.

Coronal, sagittal and axial planes are referred as to control new limb alignment of each implant components. In coronal plane both the femoral and tibial components are fixed with reference to the mechanical axis of respective bones. The alignment positions are depending on the articulating plane which is referred to mate the femoral component with the tibial polyethylene plate. In the coronal plane, the accuracy of the articulating plane is decided by femoral and tibial cut lines. If FMA is making an angle 90^0 with articulating plane, then it is known as normal alignment otherwise it develop varus and valgus deformities as shown in Fig. 2(b) and Fig. 2(c) respectively [16]. These can be partially overcome by releasing or tightening the ligaments [7]. It is also equally important if the knee is at 90^0 flexion, the co - linearity of femoral head, knee and ankle all should lay within the sagittal plane.

1.3. Need for Analysis of Limb Alignment

Surgeon's desire is to produce ideal limb alignment in coronal plane [17]. Precise component alignment in both the anterio-posterial and lateral planes is essential for proper implant function and longevity in TKR [2]. The increase in demand of TKR leads to more demand for accuracy in the alignment to improve the corresponding future results [8]. Limb alignment has been studied clinically. Alignment range $\pm3^0$ improves longetivity of total knee arthoplasty. It is hypothesis, as $\pm3^0$ is an arbitrary value; therefore need validation [9,12,14,17]. For particular conditions induced stresses in different alignment positions of varus and valgus is not found in the present literature and also its relative comparison with each other. The main objective of this work is to analyze relative pressure changes in TKR implant interface, if alignment is within the range of $\pm3^\circ$ and also if this range is increased. Optimum alignment angle may further reduce the time for ligament balancing. In such hypothesis, limb alignment analysis is utmost important to emphasize on evidence based good limb alignment position in TKR. The work flow framework is shown in Fig. 3.

2. 3D MODELLING OF BONES AND IMPLANTS

2.1. Knee Implant Modeling

2.1.1. Knee implants modeling framework

3D geometrical models were obtained by reverse engineering point cloud method. Laser scanner was used

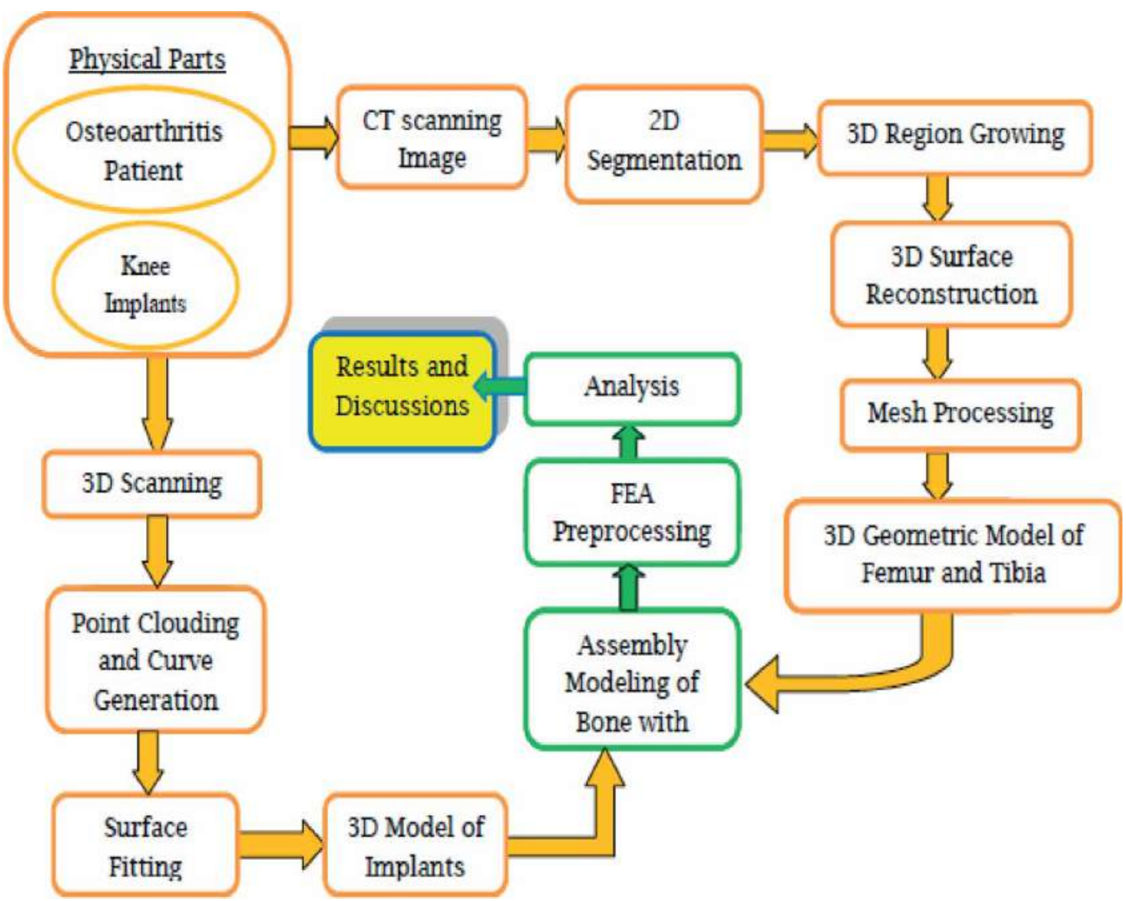

Fig. 3: Analysis of limb alignment work flow framework.

to digitize the prosthesis components. The framework shown in Fig. 4 followed to acquire the three dimensional models of implants. Knee replacement implants were selected on basis of availability of physical parts for research work considering the actual specific knee dimensions of patient.

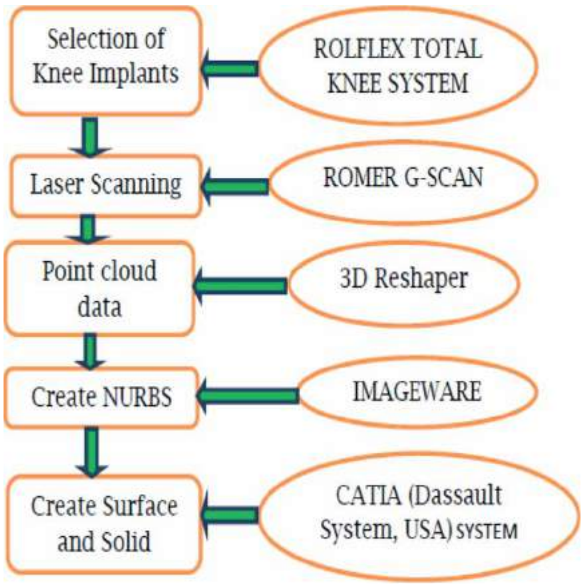

Fig. 4: Framework of 3D solid model development of prosthesis component.

2.1.2. *Data collection*

The implants were scanned by ROMER arm having capacity of its kind among CMM. 3D laser scanners are also active scanner that use laser light to probe the environment. With respect to time-of-flight of 3D laser scanner, the triangulation laser shines a laser on the subject and exploits a camera to look for the location of the laser dot. Depending on how far away the laser strikes a surface, the laser dot appears at different places in the camera's field of view. This is called triangulation technique because the laser dot, camera and the emitter form a triangle.

The length of one side of the triangle, the distance between the camera and the laser emitter were known. The angle of camera corner was determined by looking at the location of the laser dot in the camera' field of view. These three pieces of information fully determine the shape and size of the triangle and gives the location of the laser dot corner of the triangle as shown in Fig. 5.

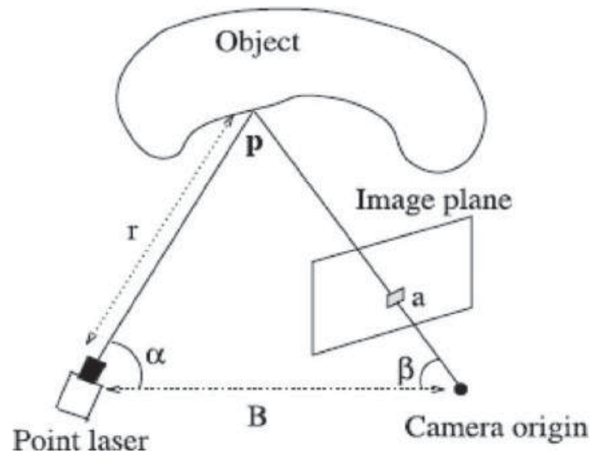

Fig. 5: Simplified data collection process [13].

By means of this technique, cloud point data of femoral component, tibial plate and polyethylene plate were obtained. Romotic software worked as a bridge between the Romer scanner and 3D Reshaper; which is used for collecting the cloud data of scanned object. 3D Reshaper performed for giving out 3D point cloud data. It covers the whole need in terms of point cloud process, 3D mesh and surface reconstruction. The cloud point data of implants were successfully obtained as shown in Fig. 6.

2.1.3. *3D modeling of knee implant*

Imageware point processing has the functionality to edit point cloud data captured from a 3D shape measurement system. It also removes noise from imported point cloud data and carries out merging, smoothing, sections extraction, alignment making and shape modification. Therefore Non-uniform rational basis spline (NURBS) curves were created by

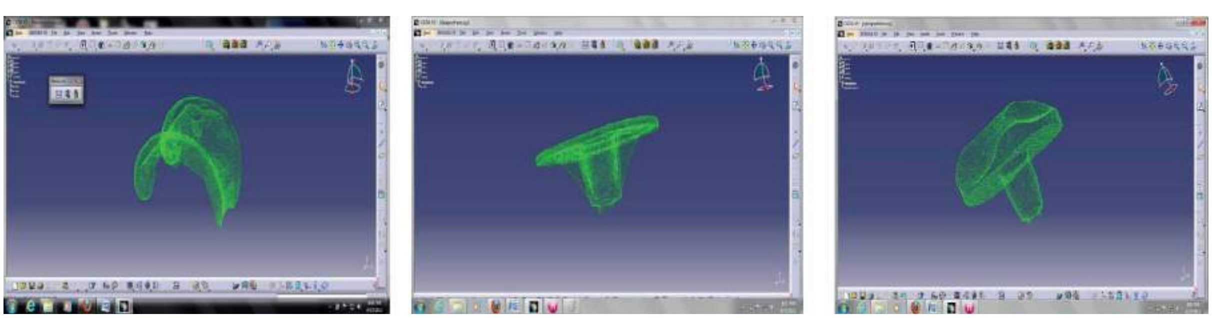

Fig. 6: Point Cloud Data of (a) Femoral Component (b) Tibial Component (c) Polyethylene Component.

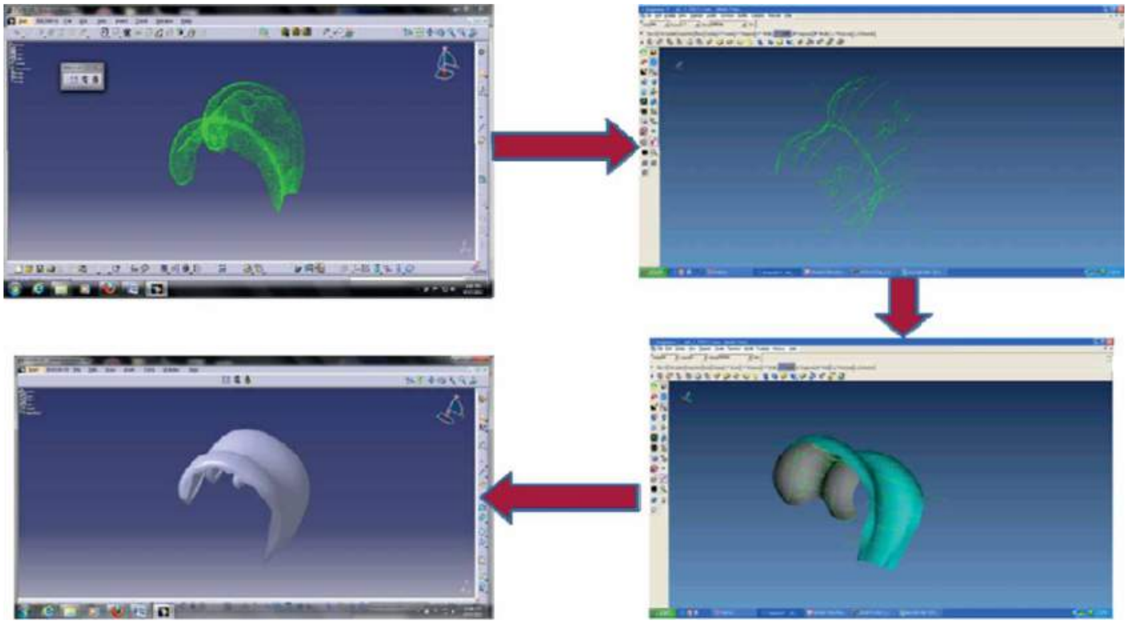

Fig. 7: 3D knee implant model generation process from point cloud data.

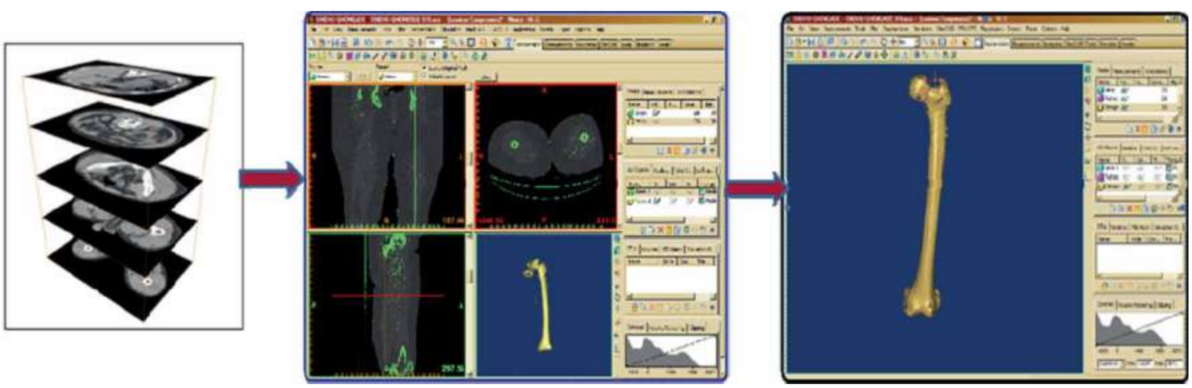

Fig. 8: Process of 3D reconstruction of bones.

taking number of section planes followed by B-spline curves. Subsequently, the polygonal surface of prosthesis was converted into solid model of femur prosthesis by generative shape editor command in CATIA as shown in Fig. 7. Similarly other two implant models were created and assembled for further analysis.

2.2. 3D Reconstruction of Bones

A female patient age of 57, suffering from the osteoarthritis and was scheduled for knee replacement surgery was identified to get the CT images. The CT images were stored in the form of DICOM (Digital Imaging and Communication in Medicine) is a standard for image exchange in digital format. CT image dataset was obtained with the femoral head to ankle joint in two sets (femur and tibia) from Toshiba - Asteion 4 Slice CT machine. An average of 862 slices were collected with resolution 512×512, field of vision = 140 mm, slice thickness = 0.5 mm, machine voltage = 120 kv and current = 100 mA. A stack of dicom files were observed in Mimics which were followed by thresholding, region growing, segmenting and editing mask finally produces the 3D bone models as shown in Fig. 8. Mimics (Materialize, Belgium) in support with 3D matic were used to reconstruct the bone. The 3D matic develop the bone models in full surface and solid form in executable commercial solid modeling format like STEP, IGES, STL etc. Similar process was carried out to obtain tibial bone model from the CT slices.

2.3. Assembly – Limb Alignment with Prosthesis

3D modeling of bones and implants were assembled together with proper reference axis generated in respective parts. The axis played vital role in assembly because it belongs to FMA and TMA. The alignment of

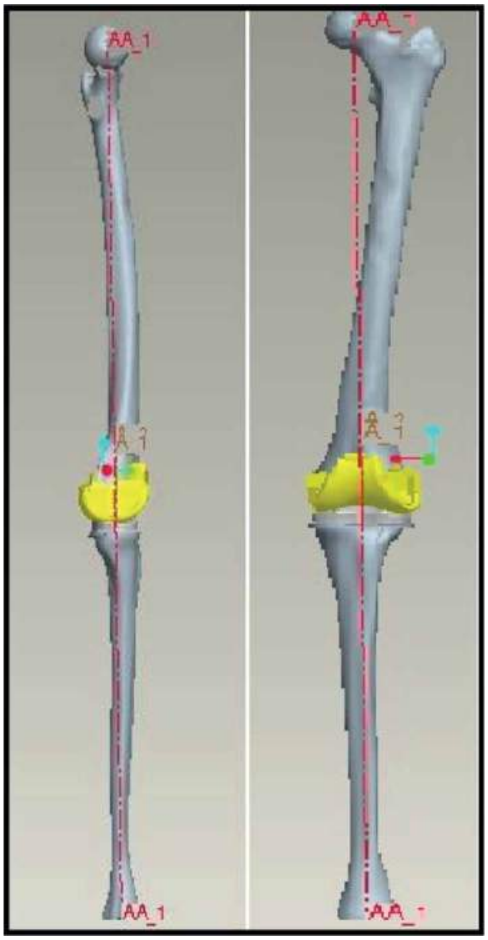

Fig. 9: Assembly model of TKR with LBA.

these axes produces the load bearing axis (LBA) where proper functionalities are expected by human knee joint. Resections of the femoral knee end and tibial knee end were performed to create a horizontal platform on which the femoral condyle and tibial baseplate rests respectively [19]. This horizontal platform actually decides the alignment angle which is also named as articulating plane or articulating interface. On the surfaces of femoral condyle and polyethylene plate required to create center points to get the axis which aligned with each other to form the LBA. The normally aligned assembly model in coronal and sagittal plane is shown in Fig. 9. Three dimensional geometrical models of varus and valgus deformities in the range of $\pm 7^0$ were created by changing the position of FMA in coronal plane. The limb alignment in TKR modeling is done in ProE wildfire (Parametric technology).

3. FINITE ELEMENT INVESTIGATION

Orthopaedic prosthesis is intended to support forces and it must be attached to the limbs. The implants are fixed into the bones either with or without acrylic cement with interface designated to provide the necessary grip. The developed knee replacement model was analyzed in this study without the bone cement. Total fifteen models with varus and valgus deformities were obtained for simulation. The material properties were defined for all three materials as shown in Tab. 1 [3,5,6].

Meshing of the model was done after defining the material properties and assigning each of the

Property	Femur and Tibia Bone	Implants Co-Cr-Mo	Polyethylene UHMWPE
Density (gm/cm^3)	1.1	8.29	0.945
Young's Modulus (GPa)	0.7–30	225	0.6–1.8
Yield Strength (MPa)	50–150	55	60
Poisson's Ratio	0.3	0.3	0.46

Tab. 1: Material Properties.

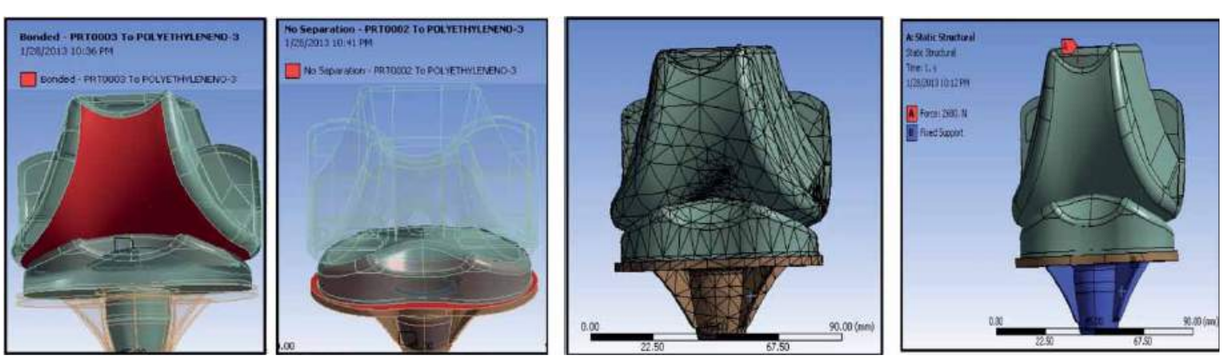

Fig. 10: FEA preprocessing with (a) bonded contact between femoral implant & Polyethylene surface (b) No separation contact between the polyethylene base and tibial top (c) Meshing and (d) Boundary conditions.

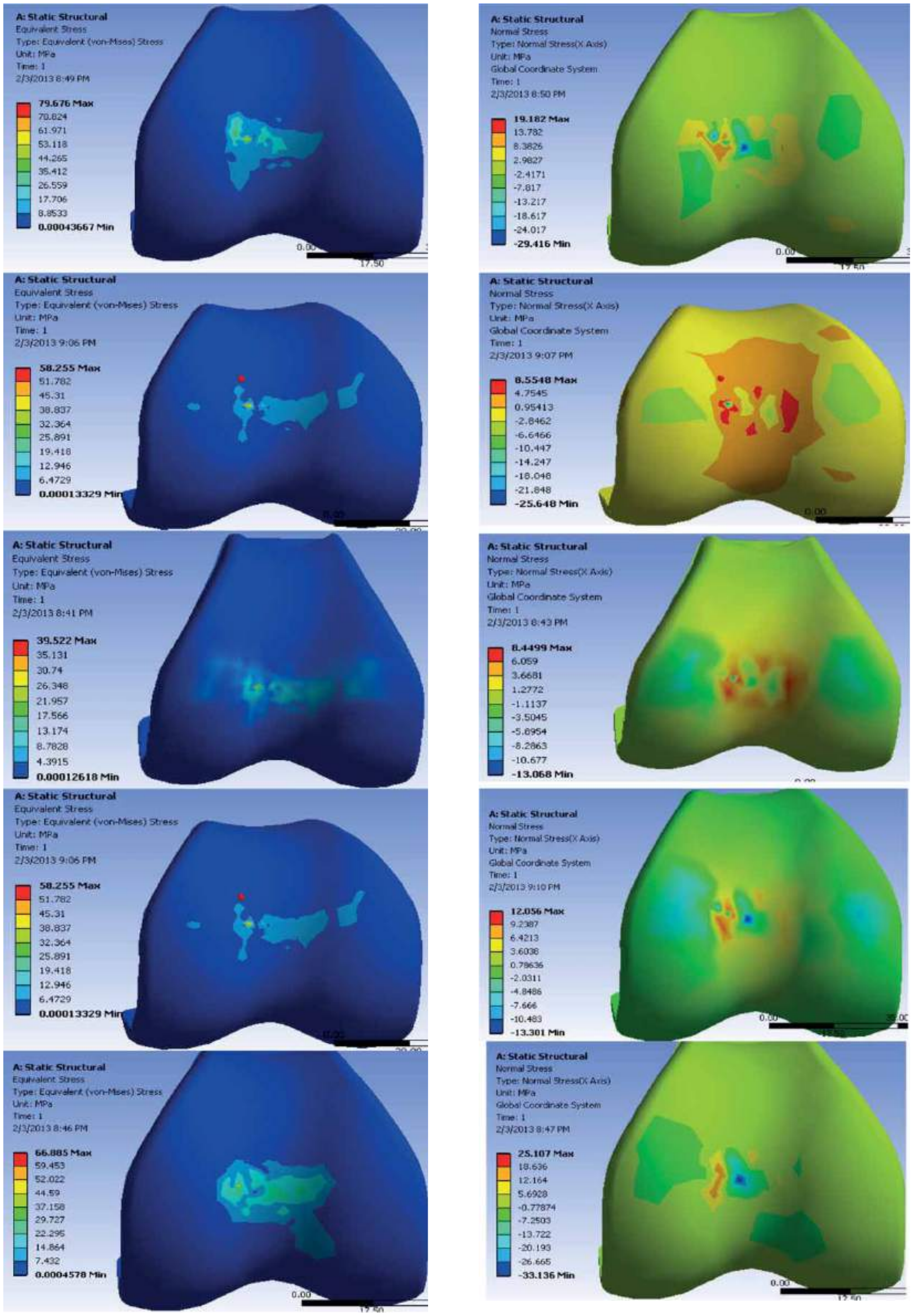

Fig. 11: Stress contours comparisons in varus 5^0, varus 3^0, 0^0 (center row) and valgus 3^0, valgus 5^0 in sequel with (a) von Mises stress and (b) Normal Stress.

Alignment Variation in Deg.	von Mises stress (MPa)	% change with Neutral value	^ Werner et al % change
7 Varus	713.210	1704.580	NR
6 Varus	506.750	1182.190	NR
5 Varus	79.676	101.599	106.301
4 Varus	46.228	16.967	NR
3 Varus	58.255	47.398	80.266
2 Varus	40.129	1.535	NR
1 Varus	39.889	0.928	NR
0 Neutral	39.522	–	–
1 Valgus	39.073	*1.136	NR
2 Valgus	43.599	10.315	NR
3 Valgus	47.793	20.927	60.993
4 Valgus	45.493	15.108	NR
5 Valgus	66.885	69.234	91.986
6 Valgus	86.727	119.430	NR
7 Valgus	86.582	119.070	NR

*Value decreases, NR = Not Reported.
^Tibial tray loading distribution with the knee in static knee extension using knee loading that would occur during trial reduction in the operating room. Pressure distribution on Medial and lateral compartments separately in tibial plate is considered with percentage comparison [20].

Tab. 2: Von Mises stress and its % change with neutral value.

components of ANSYS Workbench 14.0. The bone models were suppressed during the analysis to minimize the solution time. Triangular surface meshers was kept with program controlled and by keeping off the advanced size function to restrict the element up to 12143 and number of nodes 21170 shown in Fig. 10(c). The smoothing was kept medium and sizing relevant center option as coarse mesh selected for prosthesis. These prosthesis containing two contact surfaces defined with bonded and no separation options as shown in Fig. 10(a) and Fig. 10(b) respectively. For the static case constant force is applied, which acts while standing. While walking the load varies between 2600 N to 167 N. Hence considering the maximum load, an external force of 2600 N is applied on the top of femoral implant. 2600 N is approximately 4 time of average body weight of an individual of 60 – 65 kgs [6]. The model was fixed with all lower surfaces of tibial implant shown in Fig. 10(d).

4. RESULTS AND DISSCUSSIONS

The finite element investigation was carried out with two parameters; von mises stress and normal stress. The effect of load is observed on the surface of femoral component which is defined as the articular interface. The von Mises stress and normal stress contours are observed in Fig. 11(a) and Fig. 11(b) respectively. Initial simulation was done with the normally aligned model. Subsequently other varus and valgus alignment models were investigated up to 7^0. The result shows that with increase in the alignment deviation angle there is increase in relative stress across the articular interface. The result with von mises criterion (Tab. 2) also shows increments in the values after every 1^0 change toward varus and valgus except the 4^0 varus and valgus value. The percentage change in von Mises stress is roughly same in varus and other side there is major difference observed in the valgus alignment compared to the results obtained by Werner *et al* [20]. It is also observed that the 5^0 varus or valgus angulations greatly changed the relative stresses with a neutral alignment. The valgus alignment positions stress values are less than the varus positions. This is similar to what is believed clinically. There is sudden decrease in values of stress at $\pm 4^0$ attracts more attention and focuses on the need of further validation of these results. The exponential rise of pressure with increase in angular malposition is underlined in this study and each degree of change beyond $\pm 4^\circ$ will drastically increase pressure imbalance across articular interface and correspondingly on the tibial plate. Thus the outlier will have a drastically different pressure distribution which may affect the longevity of the implant, patient's functional capacity and revision rates.

It can also be seen that the normal stresses induced during in the contact component is increasing towards more misalignments except the value at one degree varus shown in Tab. 3. This decline value at one degree varus needs to be more focus. This study has few disadvantages. The virtual modeling is in a static mode and does not take into account the dynamic pressure situations in a real total knee replacement. Also factors like ligament laxity and soft tissue strength cannot be accounted for in the virtual model.

Alignment Variation in Deg.	Normal Stress (MPa)
7 Varus	72.472
6 Varus	36.618
5 Varus	19.182
4 Varus	13.575
3 Varus	8.554
2 Varus	8.926
1 Varus	*8.246
0 Neutral	8.449
1 Valgus	8.558
2 Valgus	9.247
3 Valgus	12.056
4 Valgus	13.768
5 Valgus	25.107
6 Valgus	32.784
7 Valgus	43.341

Tab. 3: Normal stress.

5. CONCLUSIONS

The geometrical models of bones and implants were created from the computer tomography data and point cloud approach respectively. The model investigates that the von Mises criterion, normal stress vary across the components in different alignment positions. Within $\pm 4^\circ$ the rise in stress across the model surfaces is not much; however beyond $\pm 5^\circ$ the relative pressure distribution across the articular interface drastically rises to show the pressure imbalance with every degree of change. This investigation is valuable for surgeons in TKR surgeries and possibly underlines the importance of use of computer assisted surgeries to obtain more accurate alignment and more ever to avoid the outliers outside $\pm 5^\circ$.

REFERENCES

[1] Bargren, J.-H.; Blaha, J.-D.; Freeman M.-A.: Alignment in total knee arthoplasty: correlated biomedical and clinical investigations, Clinical Orthopedics and Related Research, 1983, 173–178.

[2] Bono, J.; Chapter12: Tibial alignment, Revision of total knee arthoplasty, 129–136.

[3] Carr, B.-C.; Goswami, T.: Knee implants – Review of models and biomechanics, Materials and Design 30, 2009, 398–413.

[4] Derek, T. -V.; Cooke, U; Kelly Brian; Li Jian.: Prosthetic reconstruction of the arthritic knee: considerations for limb alignment, geometry and soft tissue reconstruction, The Knee, 5, 1998, 165–174.

[5] E28 5231- 11/09 Manual, Evolutis, France.

[6] Ghyar, R.; Ravi, B.; Anasane, S.; Pandey, A.; Karnik, S.; Shetty, A.: Static and Dynamic Analysis of Tumor Knee Prosthesis, 4th India/ASEAN Hyperworks technology Conference, Bangalore, India, July 31-Aug 2, 2008.

[7] Hood, R.; Vanni, M.; Insal, J.: The correction of knee alignment in 225 consecutive total condylar knee replacements, Clinical Orthopedics and Related Research 160, 1981.

[8] Longstaff, L.-M.; Sloan, K.; Stamp, N.; Scaddan, M.; Beaver, R.: Good alignment after total knee arthoplasty leads to faster rehabilitation and better function, Journal of Orthoplasty, 24(4), 2009.

[9] Maniar, R.; Johorey, A.; Pujary, T.; Yadava, A.: Margin of error in alignment: a study undertaken when converting from conventional to computer-assisted total knee arthoplasty, Journal of Arthoplasty, 26(1), 2011.

[10] Matsuda, S.; Miura, H.; Nagamine, R.; Urabe, K.; Harimaya, K.; Matsunobu, T.; Iwamoto, Y.: Changes in knee alignment after total knee arthoplasty, Journal of Orthoplasty, 14(5), 1999.

[11] Mohanlal, P.; Jain, S.: An analysis of intraoperative variation in femorotibial alignment in the coronal plane during computer navigated total knee replacement, Acta Orthop. Belg., 2010, 76, 233–236.

[12] Moreland, J.: Mechanisms of failure in total knee arthoplasty, Clinical Orthopedics and Related Research, 226, 1988.

[13] Page, D.; Koschan, A.; Sun, Y.; Abidi, M.: Laser-based imaging for reverse engineering, Sensor Rev. 23, 2003, 223–229.

[14] Patel, D.-V.; Ferris, B.-D.; Aichroth, P.-M.: Radiological study of alignment after total knee replacement. Short radiographs or long radiographs, Int. Orthop, 15(3), 1991, 209–10.

[15] Ritter, M.-A.; Faris, P.-M.; Keating, E.-M.; Meding, J.-H.: Postoperative alignment of total knee replacement. Its effect on survival, Clin Orthop Relat Res, 1994, 299–153.

[16] Russo, A.; Laura, B.; Trozzi, C.; Stefano, Z.; Neri, M.; Bruni, D.; Marcassi, M.: Recurrence of varus/valgus deformity after TKR at 3 years' follow-up, The Knee 15, 2008, 20–25.

[17] Sikorski, J.-M.: Alignment in total knee replacement, J bone joint surg, 90-B (9), 2008.

[18] Tew, M.; Waugh, W.: Tibiofemoral alignment and the results of knee replacement, Journal of Bones and Joint Surgery, 16–4B, 1985.

[19] Wasielewsk, R.; Galante, J. –O.; Leighty, R. –M.; Natrajan, R. –N, Rosenberg, A. –G.: Wear patterns on retrieved polyethylene tibial inserts and their relationship to technical considerations during total knee arthoplasty, Clinical Orthopedics and Related Research, November 299, 1994, 31–43.

[20] Werner, F.; Ayers. D.; Maltesky. L.; Rullkoettor. P.: The effect of valgus/varus malalignment in load distribution in total knee replacements, Journal of Biomechanics, 38, 2005, 349–355.